Supporting information

Study on the influence conditions of luminescence properties of ionic $[Cu(N^N)(P^P)]^+$ complexes: ligands, counteranions and weak interactions

Zi-Xi Li,[†a] Zhen-Zhou Sun,[†a] Guo Wang,[a] Wei Yang,[b] Hong-Liang Han,[a] Yu-Ping Yang,[c] Zhong-Feng Li,[a] Lixiong Dai,*[d,e] Yi-shan Yao*[f] and Qiong-Hua Jin*[a,g]

[a]*Department of Chemistry, Capital Normal University, Beijing 100048, China. E-mail: jinqh@cnu.edu.cn*

[b]*Faculty of Food Science and Technology, Suzhou Polytechnical Institute of Agriculture, Suzhou 215008, P. R. China.*

[c]*School of Science, Minzu University of China, Beijing 100081, China.*

[d]*Wenzhou Institute, University of Chinese Academy of Sciences, Wenzhou, Zhejiang 325000, China, email: dailx@ucas.ac.cn*

[e]*Oujiang Laboratory, Wenzhou, Zhejiang 325000, China*

[f]*State Key Laboratory of Tocicology and Medical Countermeasures, Beijing Institute of pharmacology and Toxicology, No. 27 Taiping Road, Haidian District, Beijing, 100850, P. R. China.*

[g]*State Key Laboratory of Structural Chemistry, Fujian Institute of Research on the Structure of Matter, Chinese Academy of Sciences, Fuzhou, Fujian 350002, China.*

‡**Zi-Xi Li** and **Zhen-Zhou Sun** contributed equally to this work.

†Electronic Supplementary Information (ESI) available: crystal structure information, spectra date and computation details. CCDC: 2091103-2091105, 2091107-2091108, 2174893-2174925.

Caption of Figure

Caption of Table

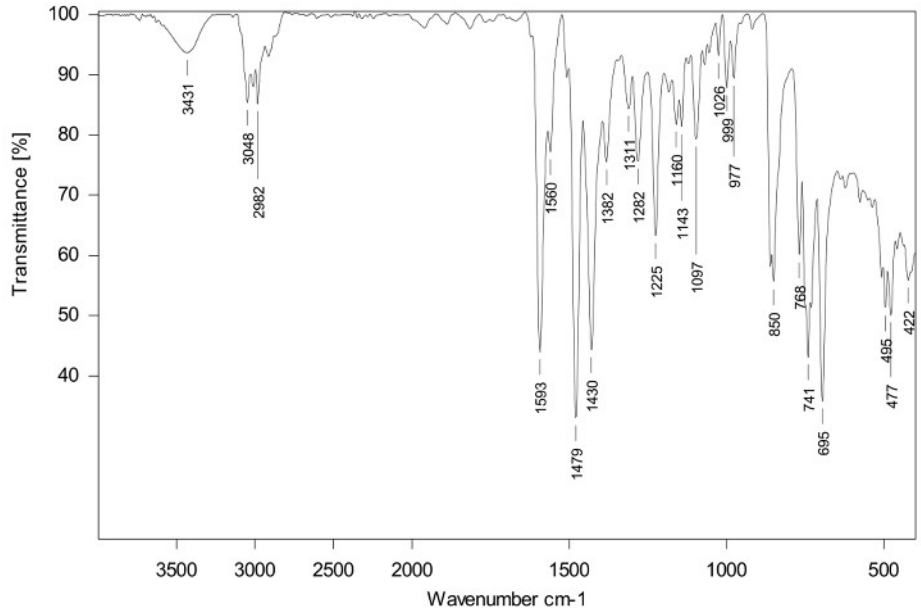

Fig. S1 The IR spectra for complex **1a**.

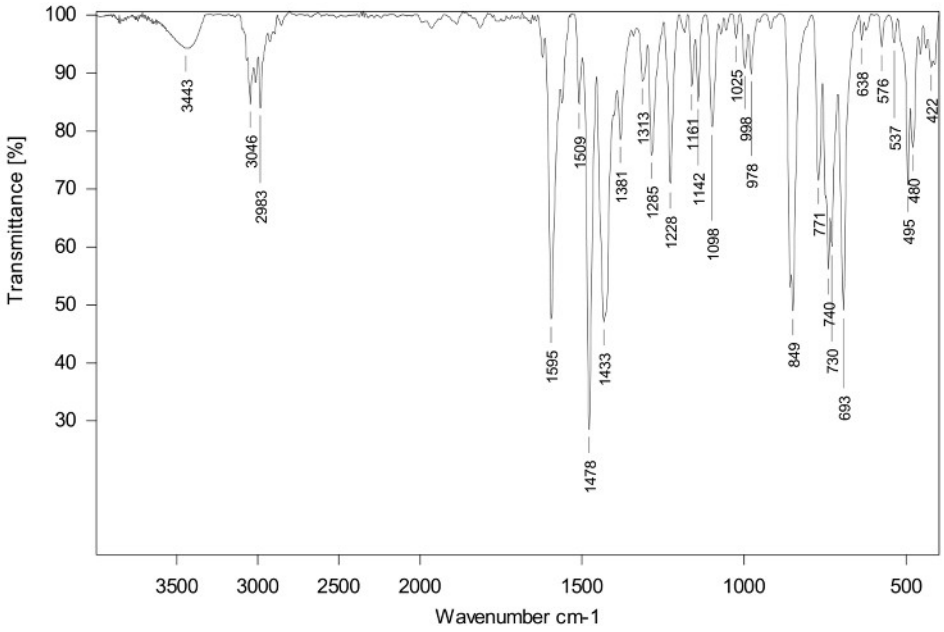

Fig. S2 The IR spectra for complex **2a**.

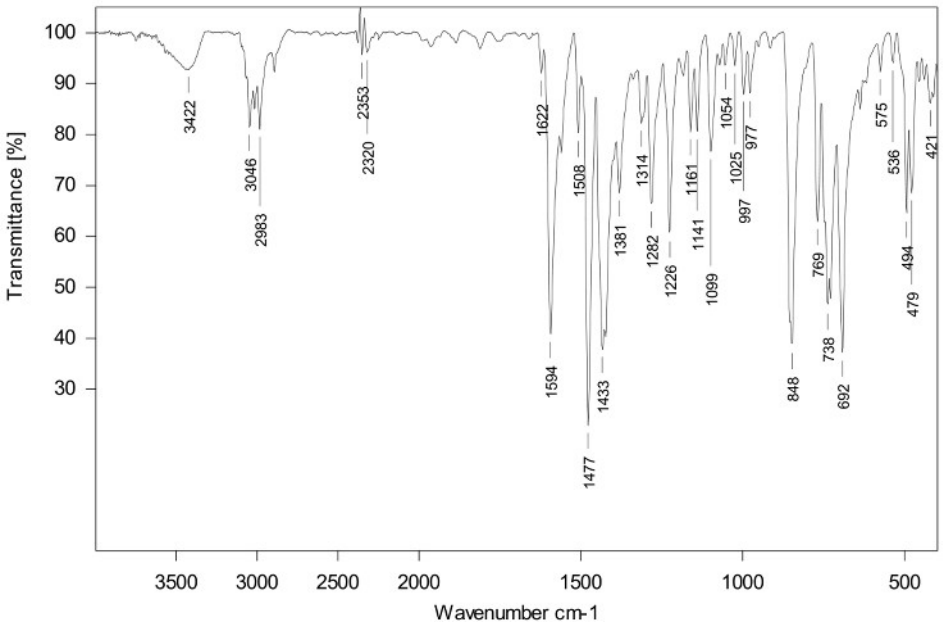

Fig. S3 The IR spectra for complex **3a**.

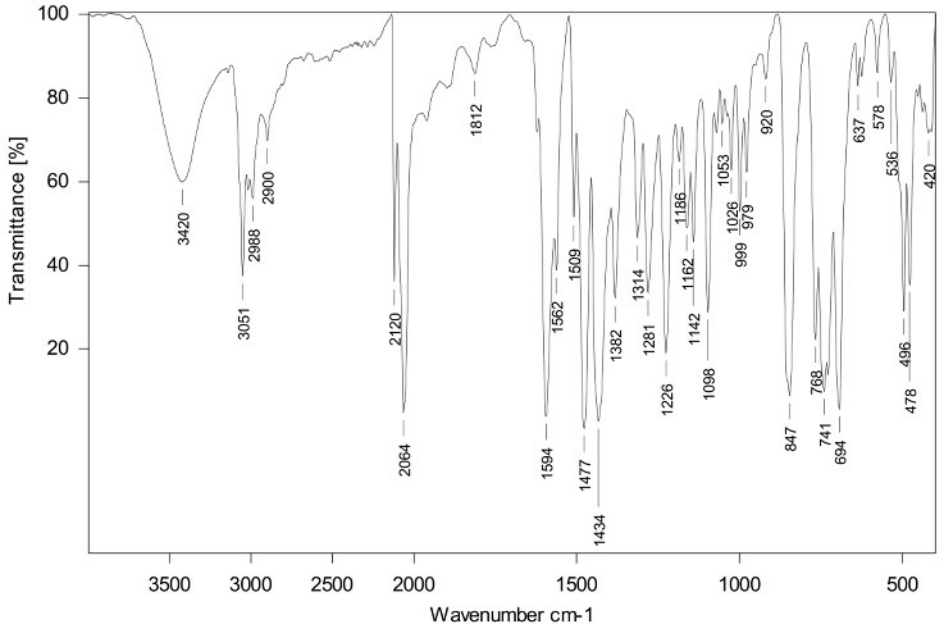

Fig. S4 The IR spectra for complex **4a**.

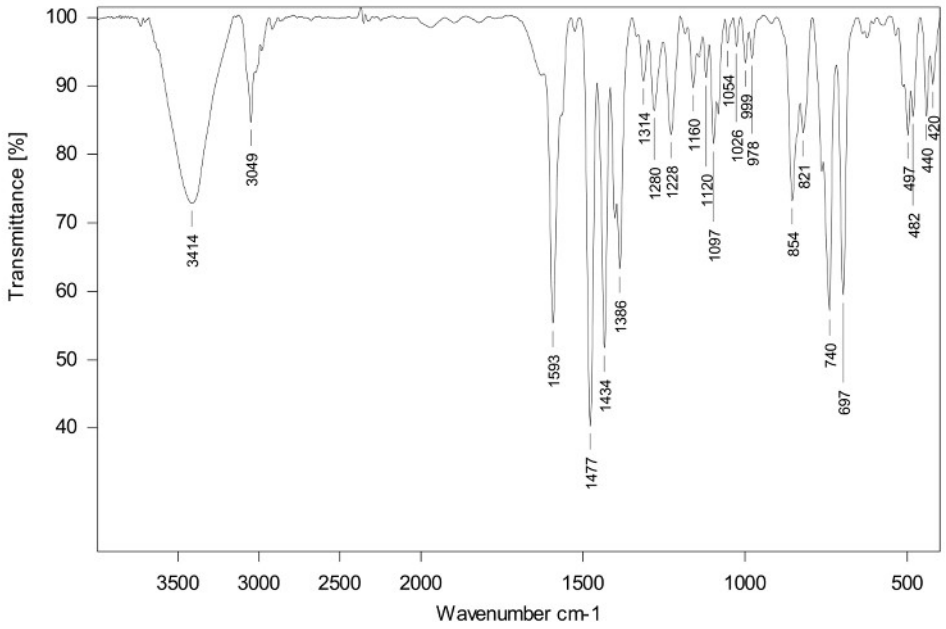

Fig. S5 The IR spectra for complex **1b**.

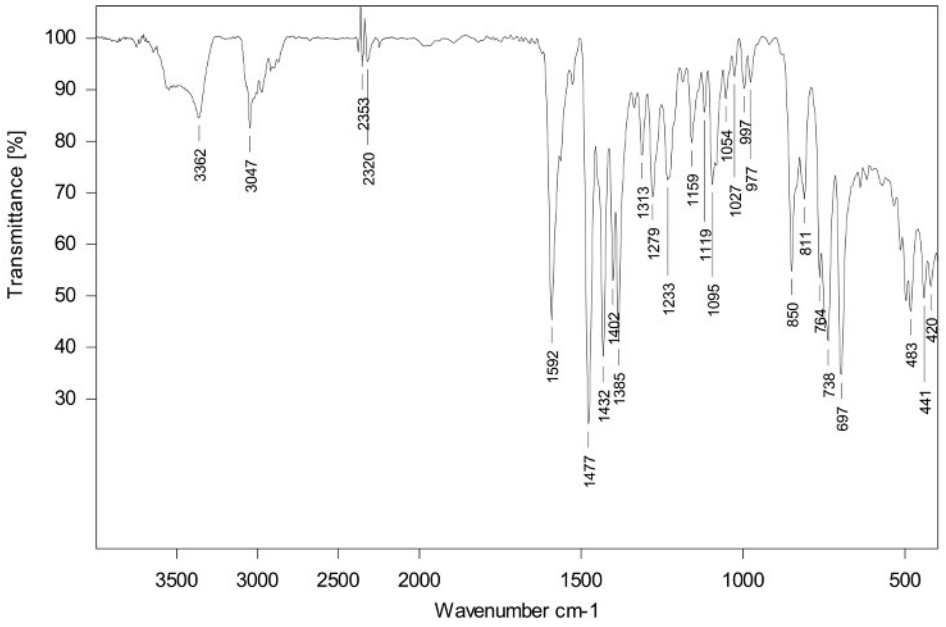

Fig. S6 The IR spectra for complex **2b**.

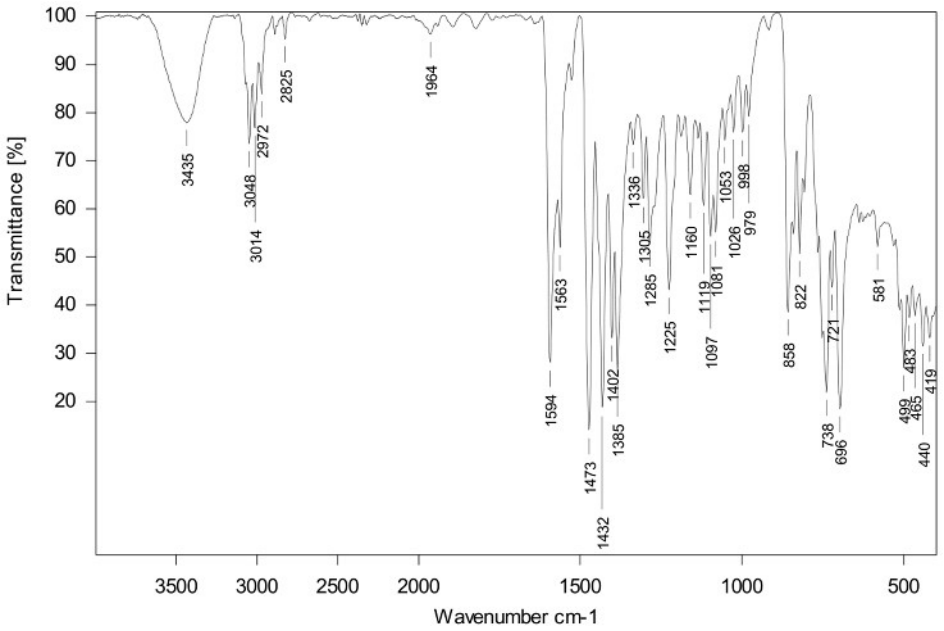

Fig. S7 The IR spectra for complex **3b**.

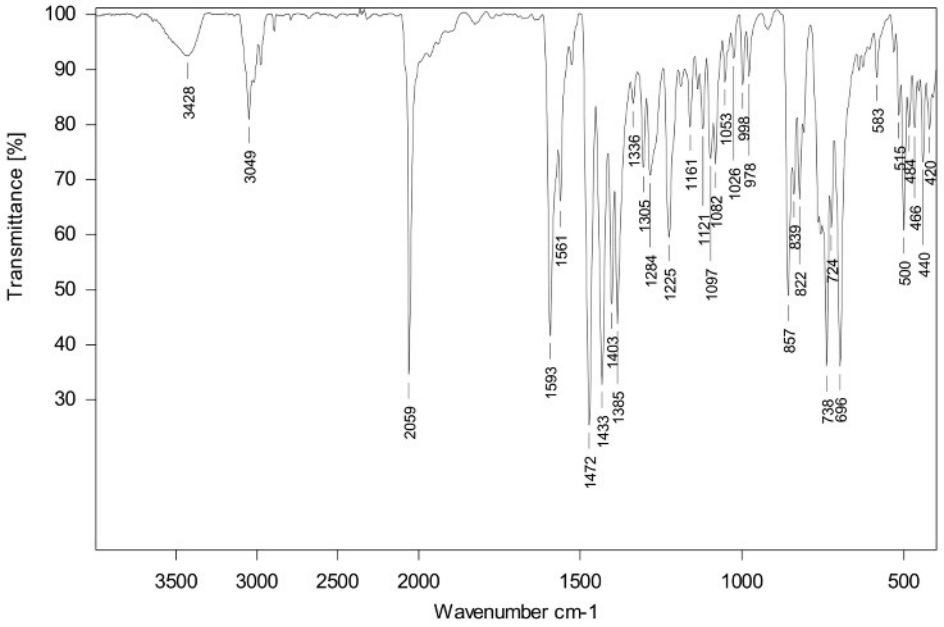

Fig. S8 The IR spectra for complex **4b**.

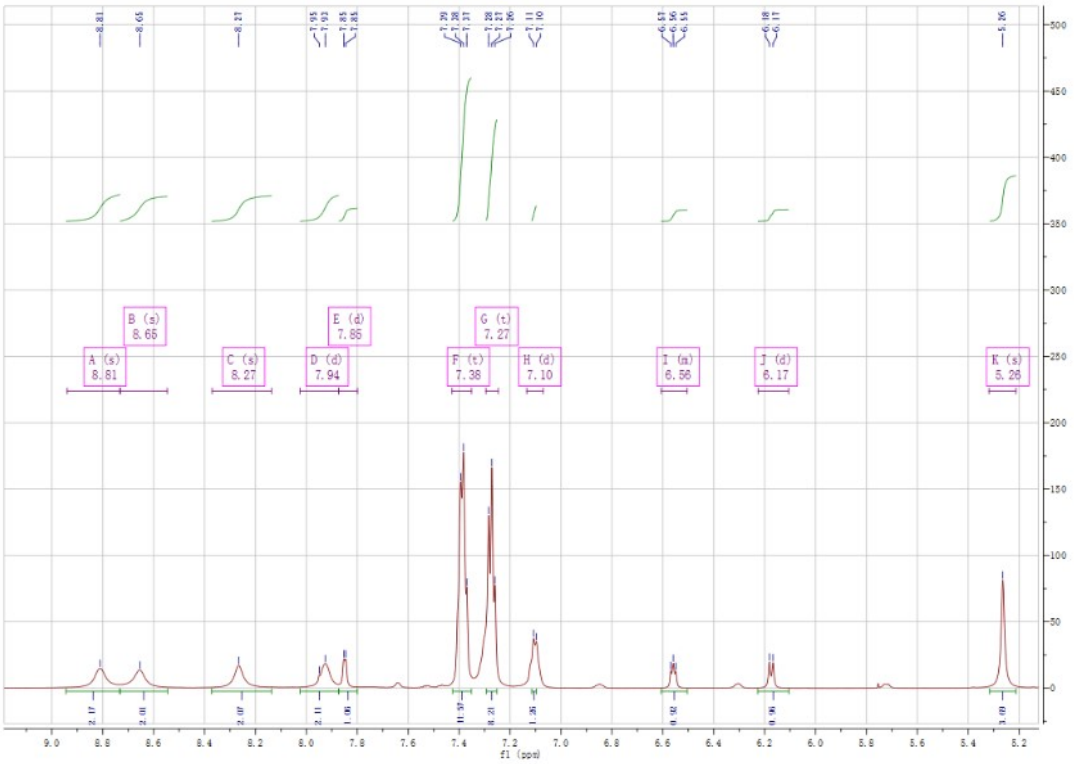

Fig. S9 The ^{1}H NMR spectra for complex **1a**.

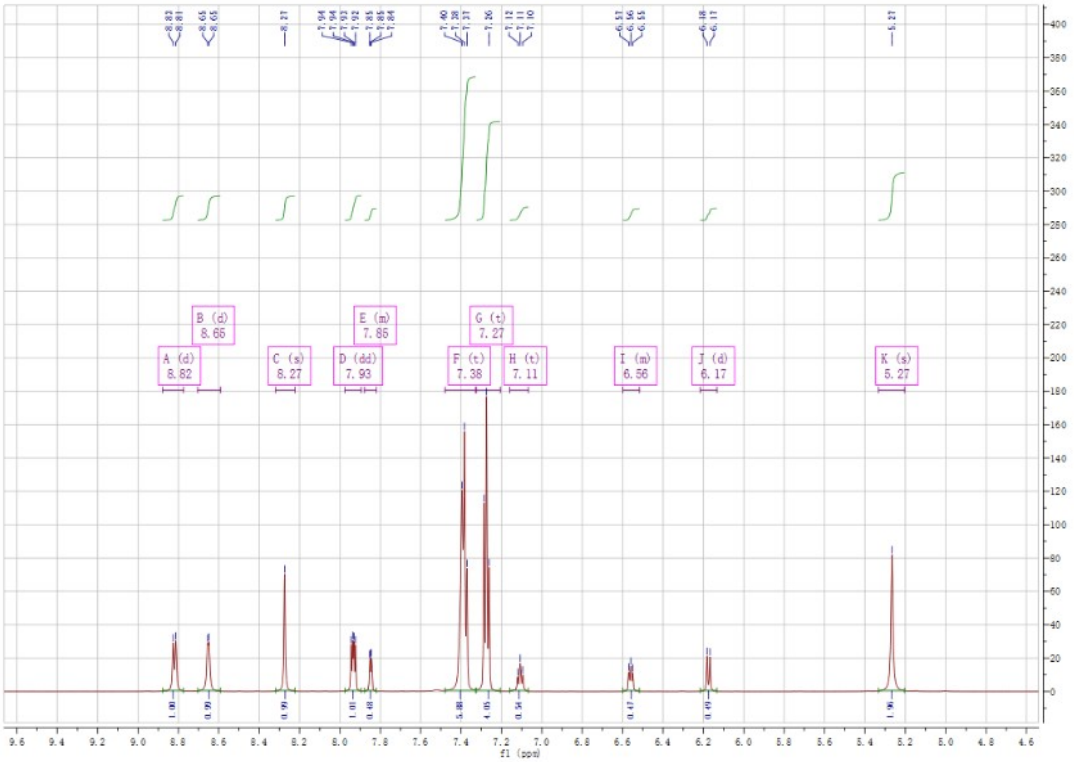

Fig. S10 The ^{1}H NMR spectra for complex **2a**.

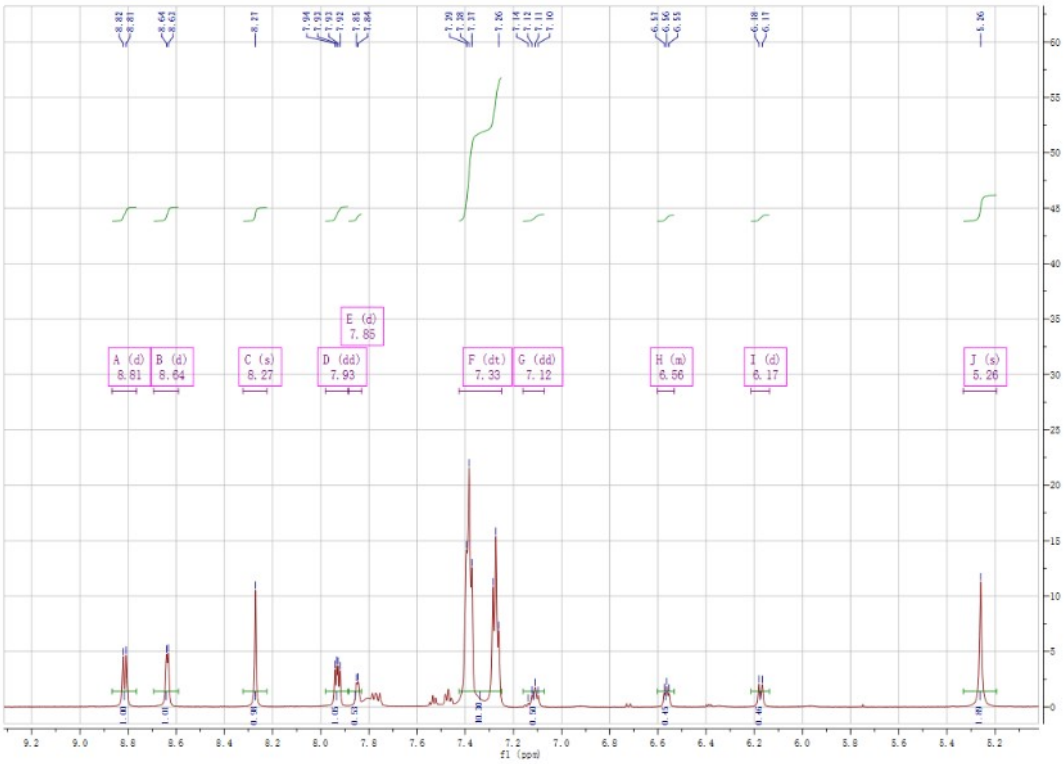

Fig. S11 The ^{1}H NMR spectra for complex **3a**.

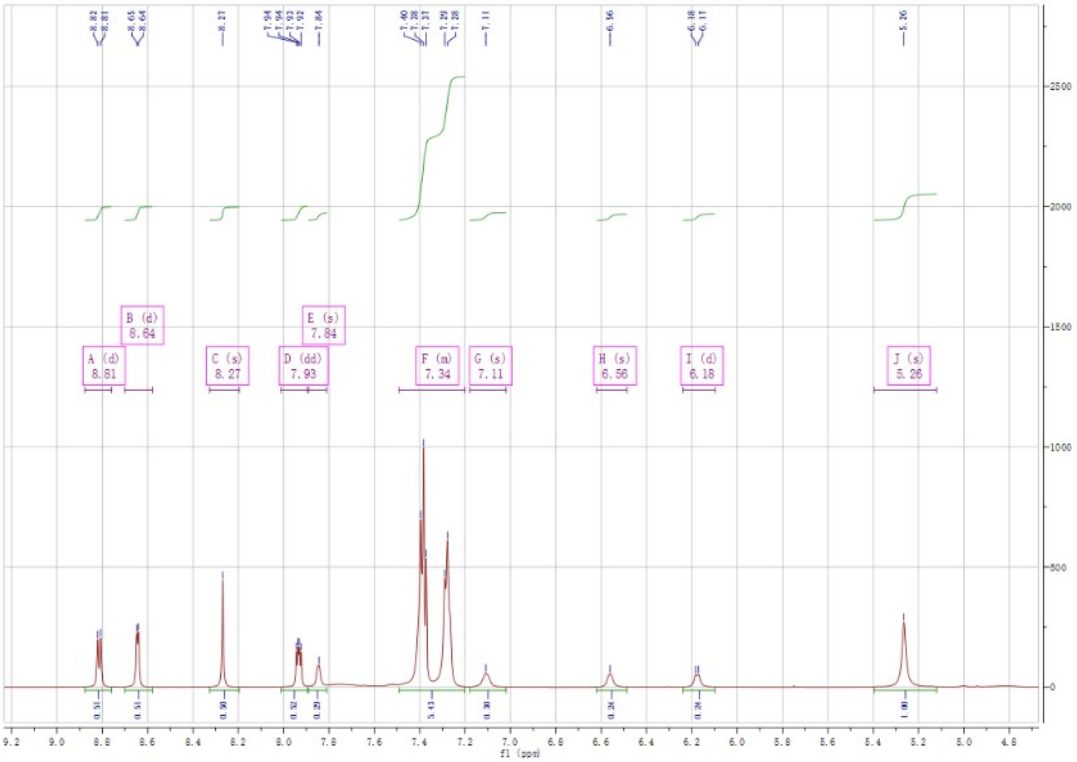

Fig. S12 The ^{1}H NMR spectra for complex **4a**.

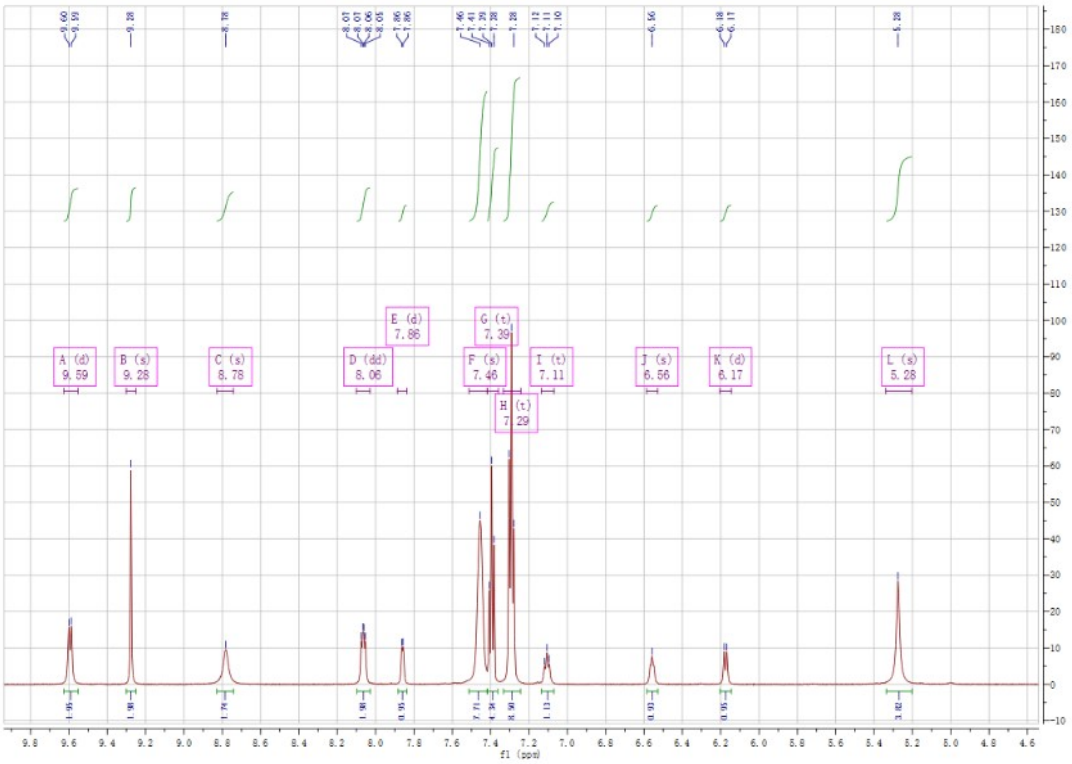

Fig. S13 The ^{1}H NMR spectra for complex **1b**.

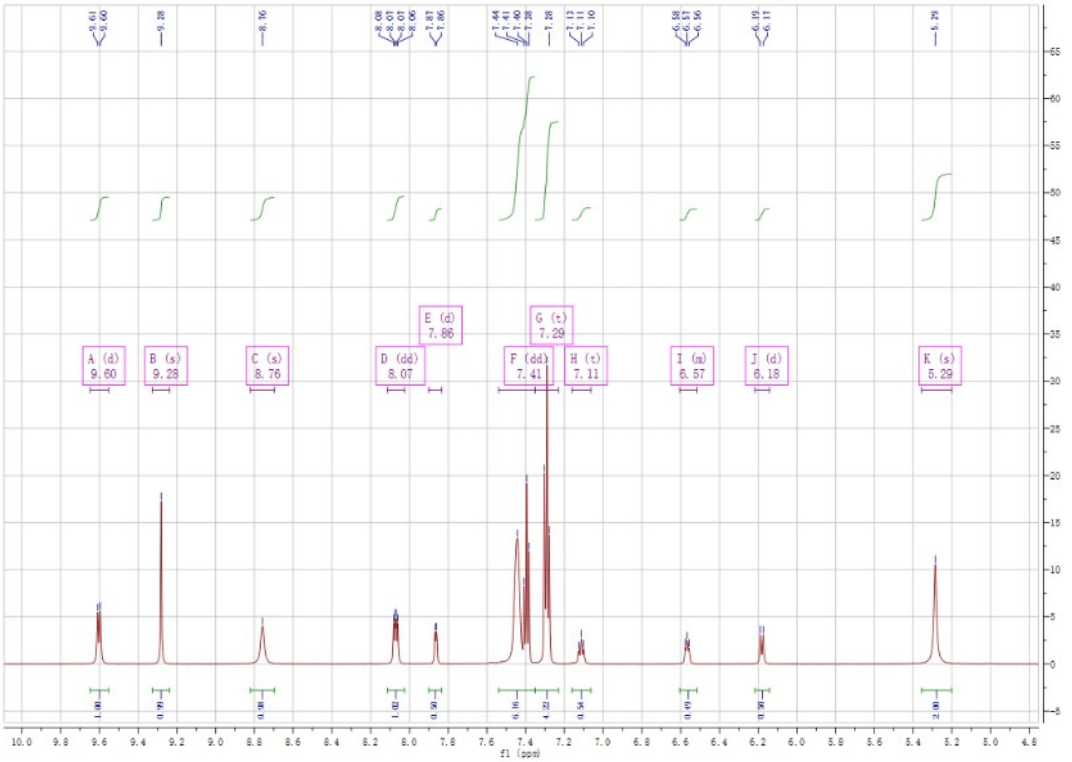

Fig. S14 The ^{1}H NMR spectra for complex **2b**.

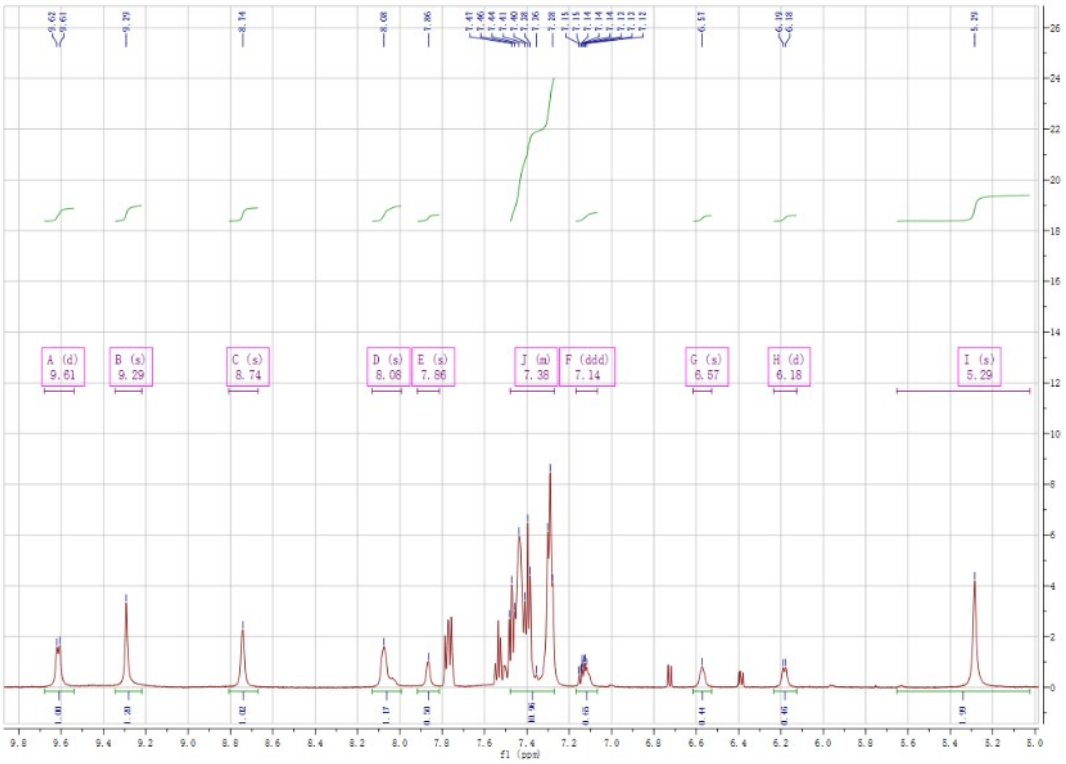

Fig. S15 The ^{1}H NMR spectra for complex **3b**.

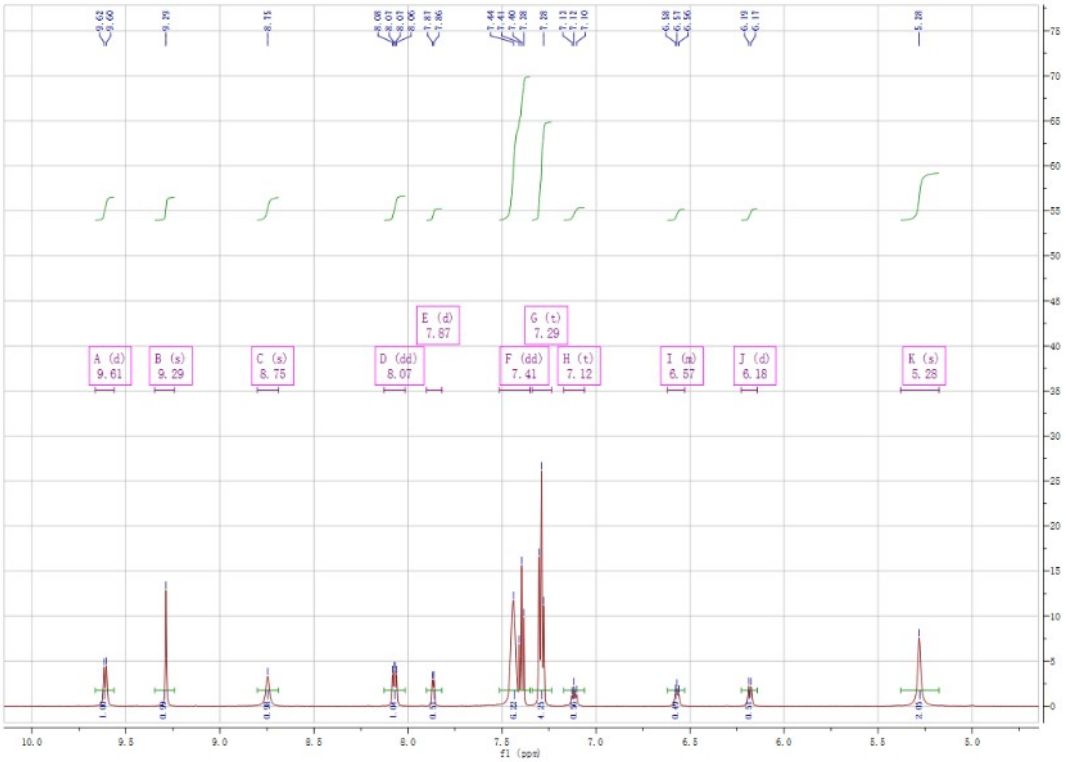

Fig. S16 The ^{1}H NMR spectra for complex **4b**.

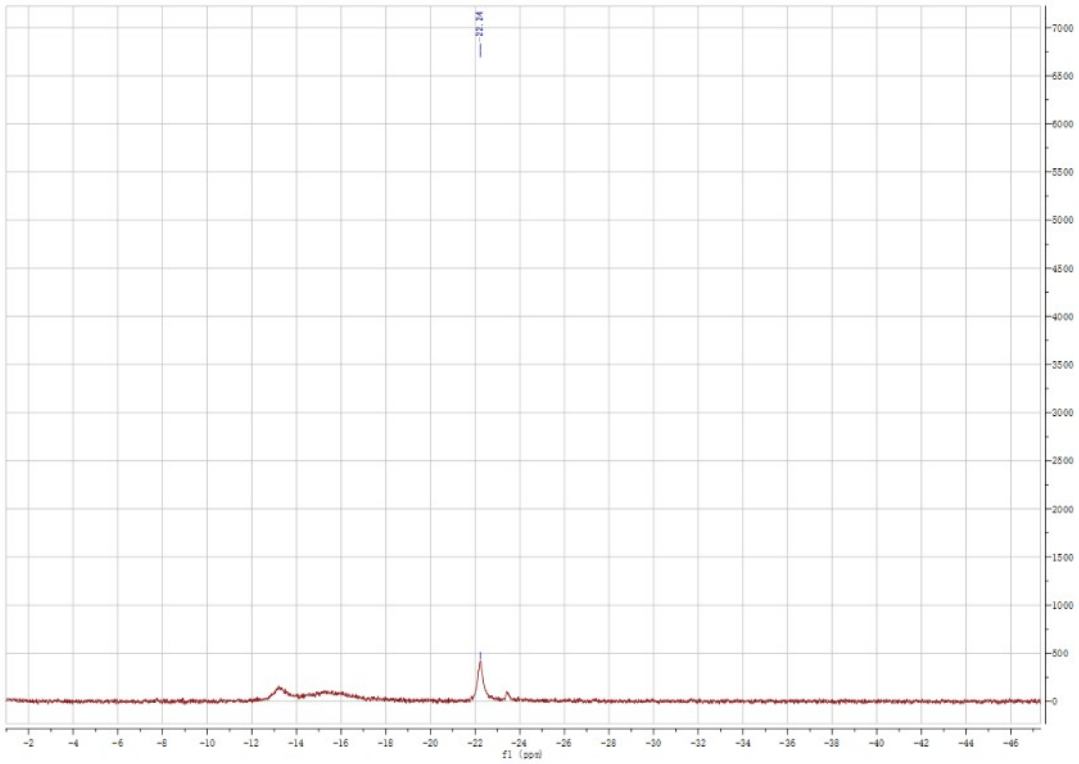

Fig. S17 The ^{31}P NMR spectra for complex **1a**.

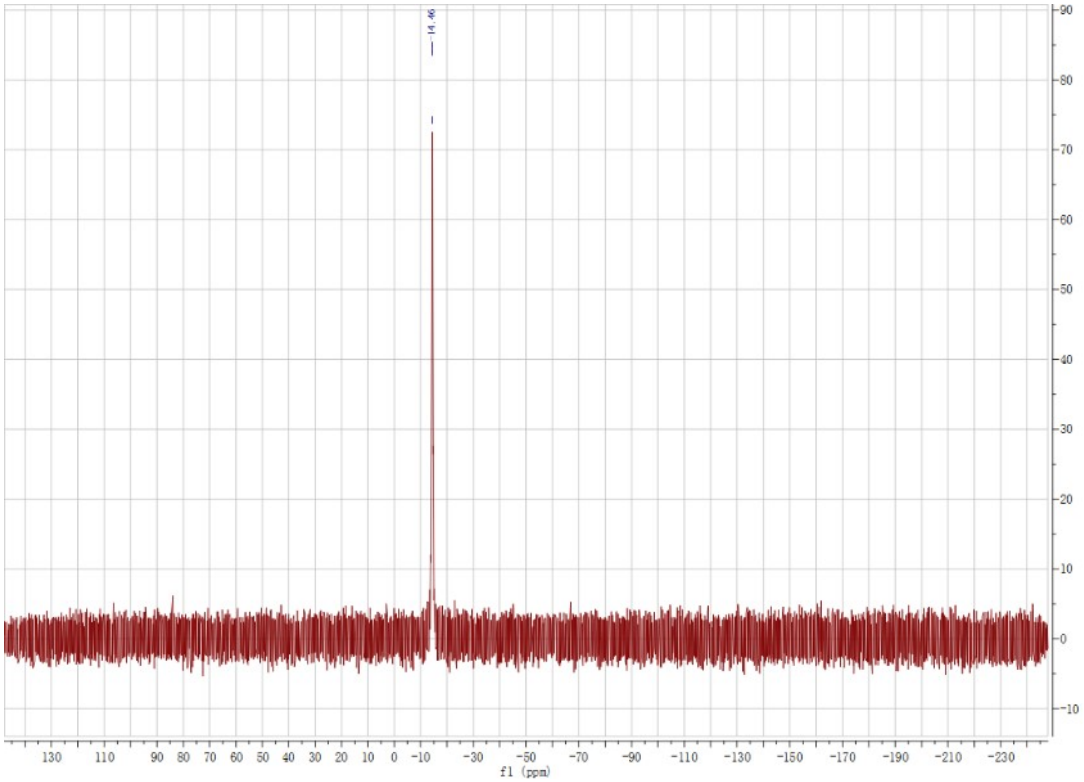

Fig. S18 The ^{31}P NMR spectra for complex **2a**.

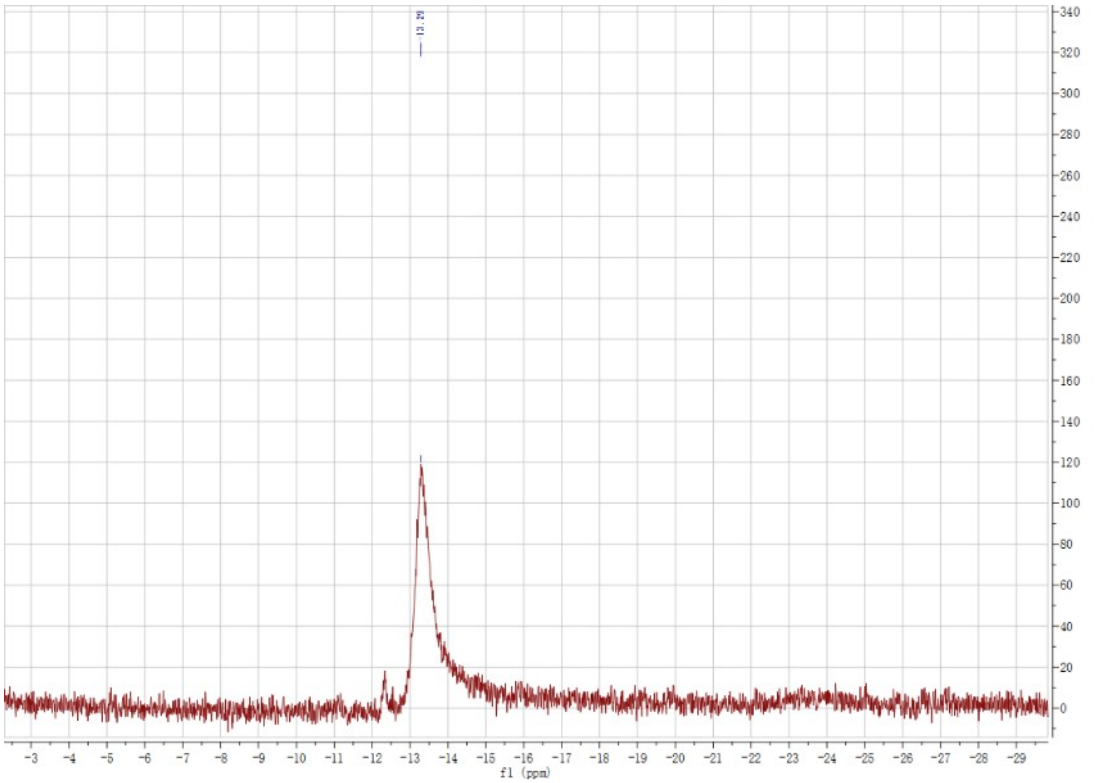

Fig. S19 The ^{31}P NMR spectra for complex **3a**.

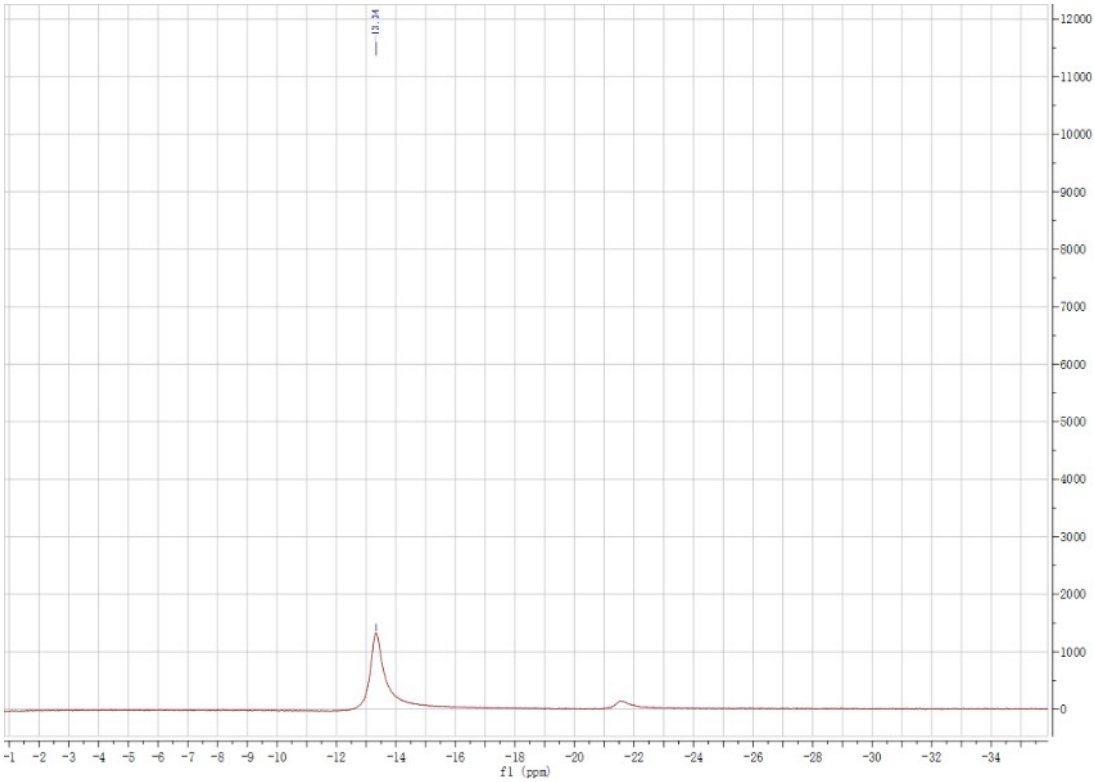

Fig. S20 The ^{31}P NMR spectra for complex **4a**.

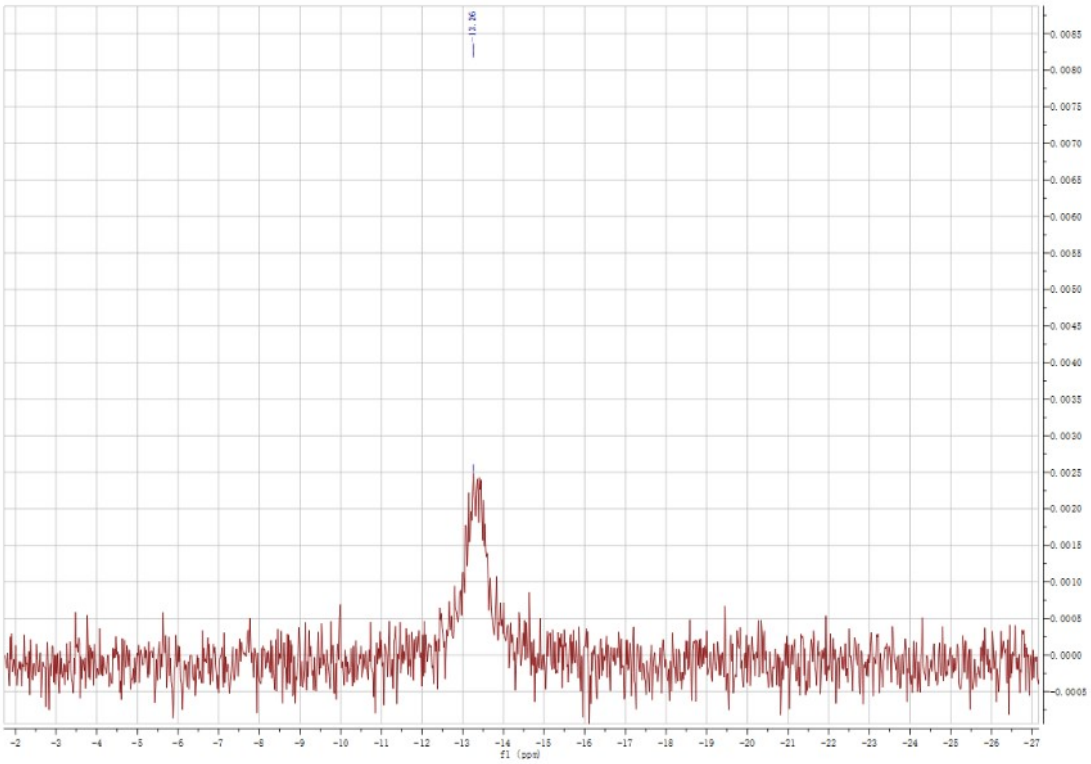

Fig. S21 The ^{31}P NMR spectra for complex **1b**.

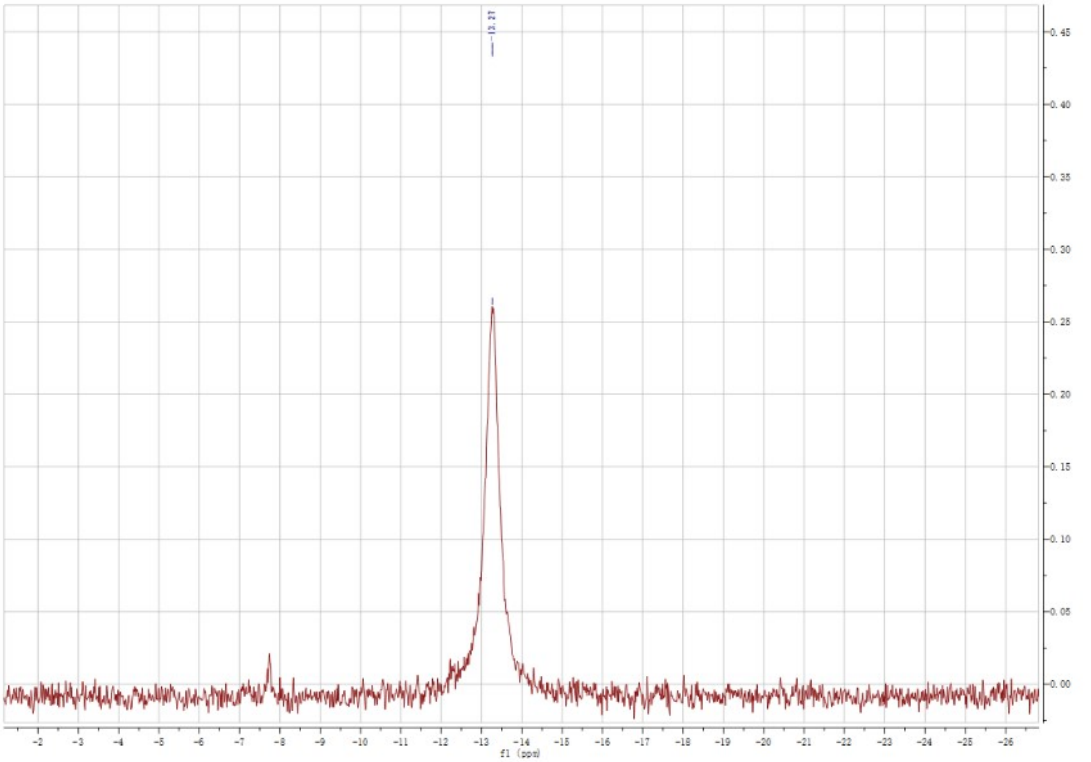

Fig. S22 The ^{31}P NMR spectra for complex **2b**.

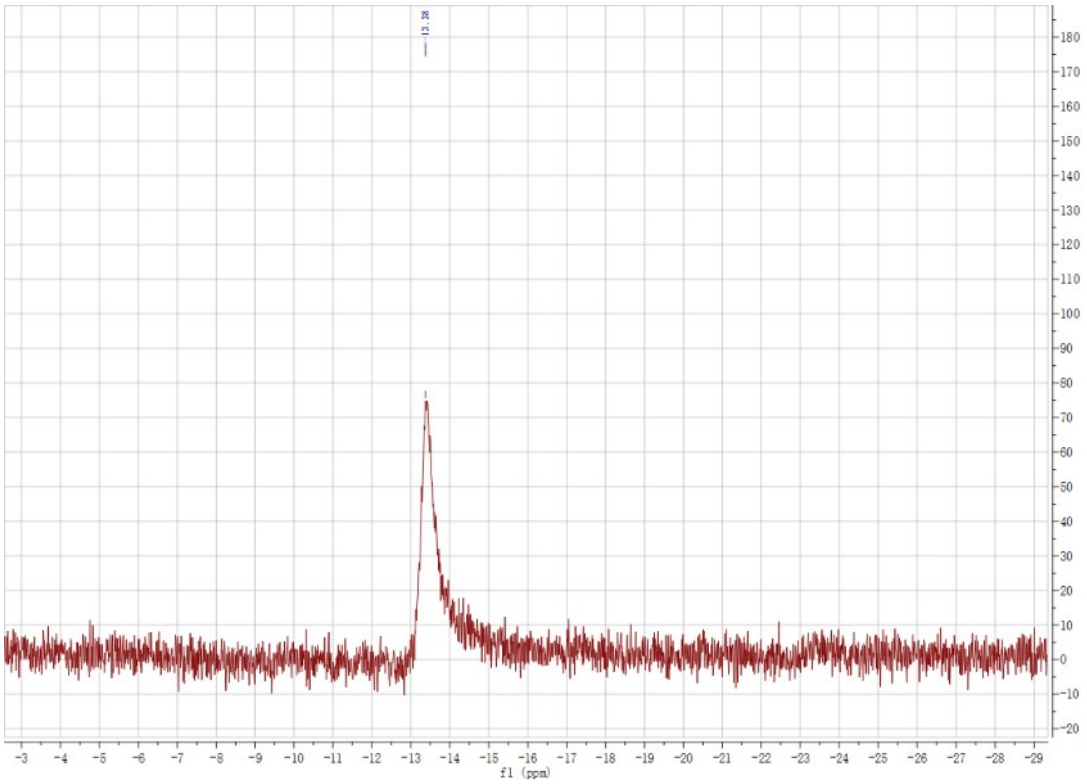

Fig. S23 The ^{31}P NMR spectra for complex **3b**.

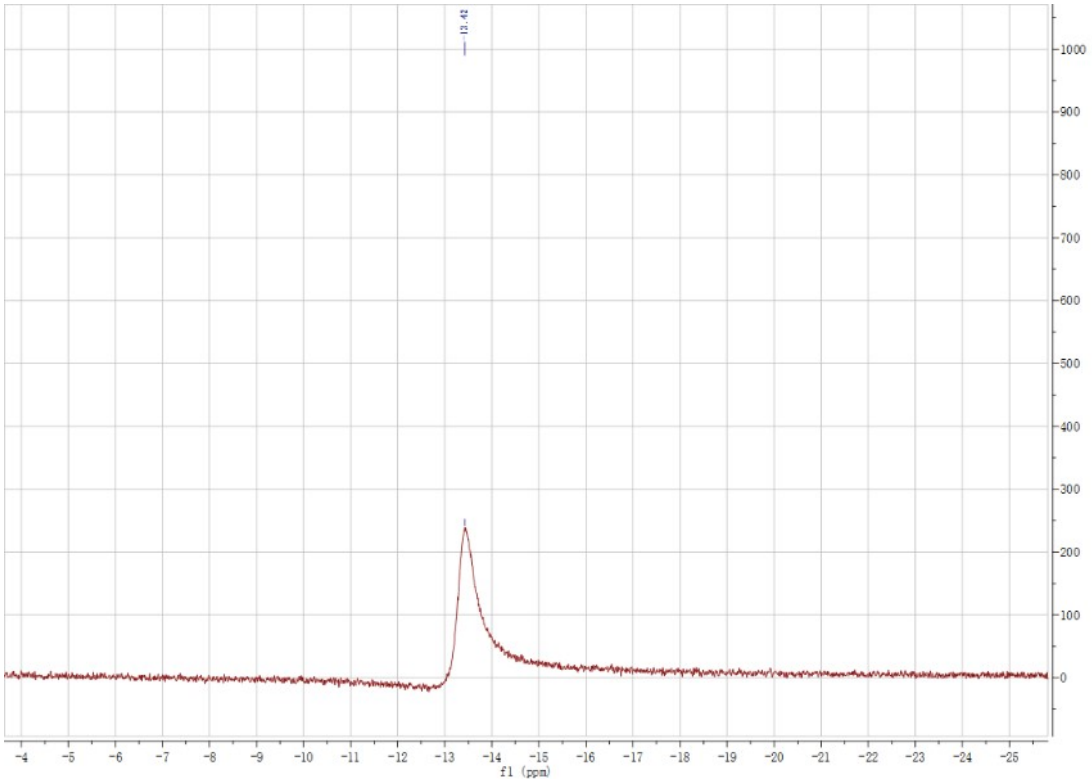

Fig. S24 The ^{31}P NMR spectra for complex **4b**.

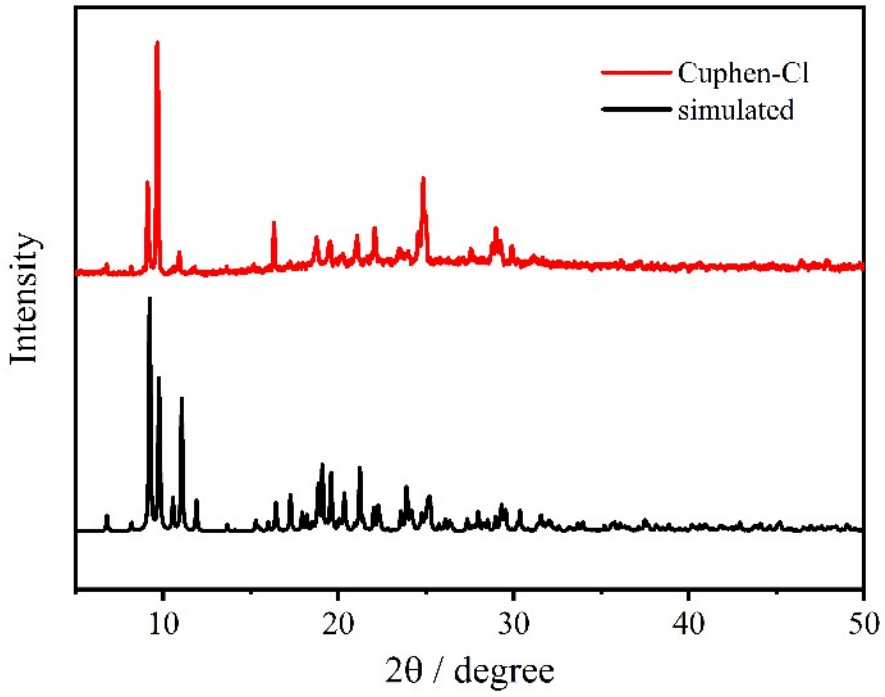

Fig. S25 The PXRD patterns for complex **1a**: simulated from single crystal data (Black) and single phase polycrystalline sample (Red).

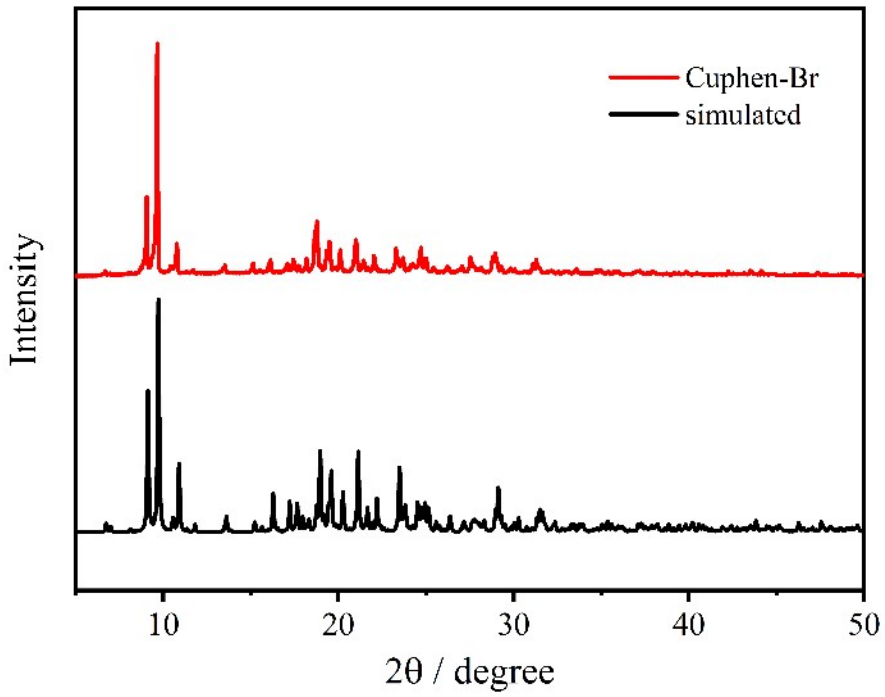

Fig. S26 The PXRD patterns for complex **2a**: simulated from single crystal data (Black) and single phase polycrystalline sample (Red).

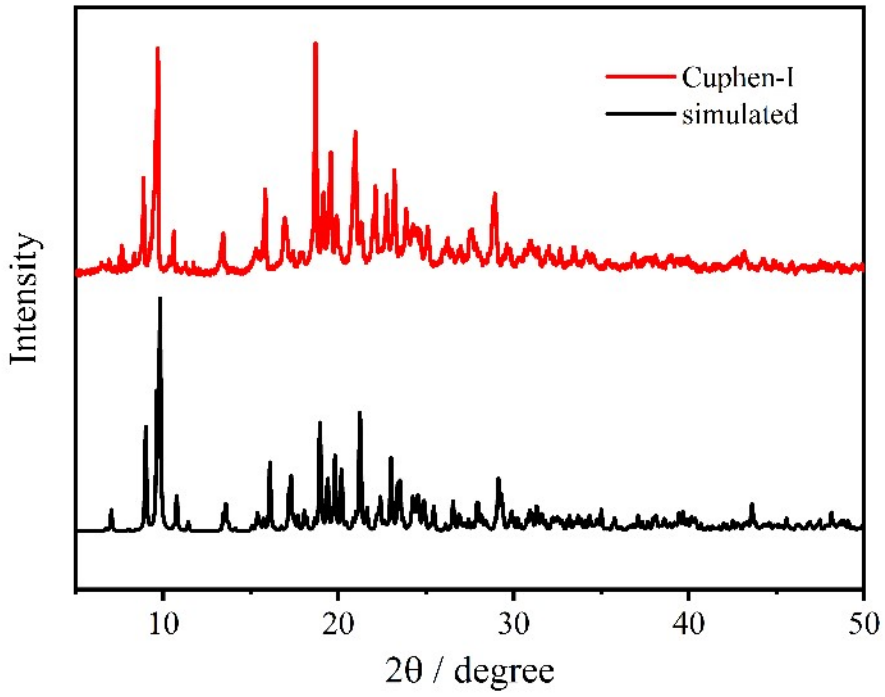

Fig. S27 The PXRD patterns for complex **3a**: simulated from single crystal data (Black) and single phase polycrystalline sample (Red).

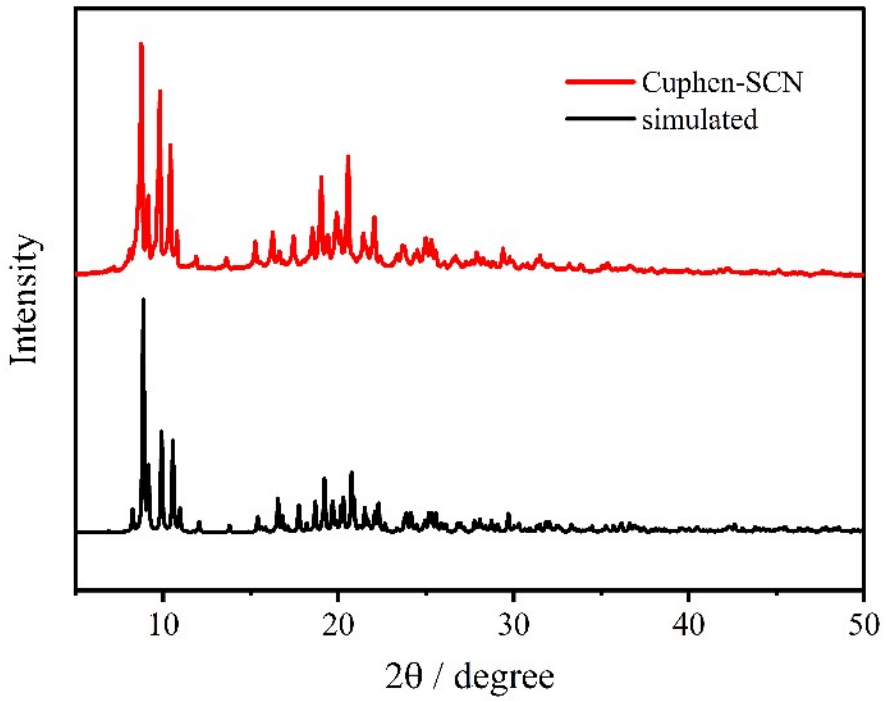

Fig. S28 The PXRD patterns for complex **4a**: simulated from single crystal data (Black) and single phase polycrystalline sample (Red).

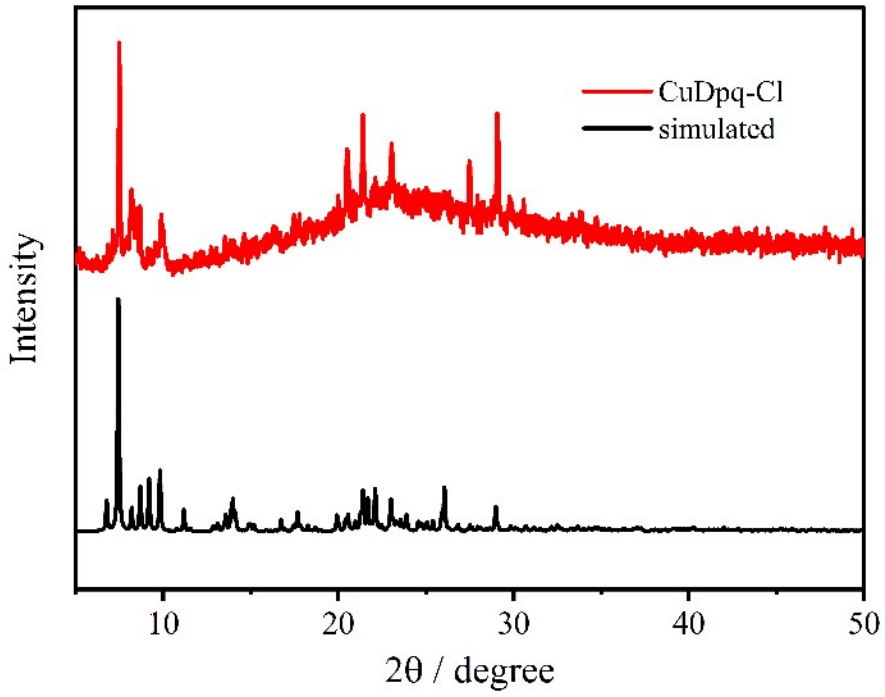

Fig. S29 The PXRD patterns for complex **1b**: simulated from single crystal data (Black) and single phase polycrystalline sample (Red).

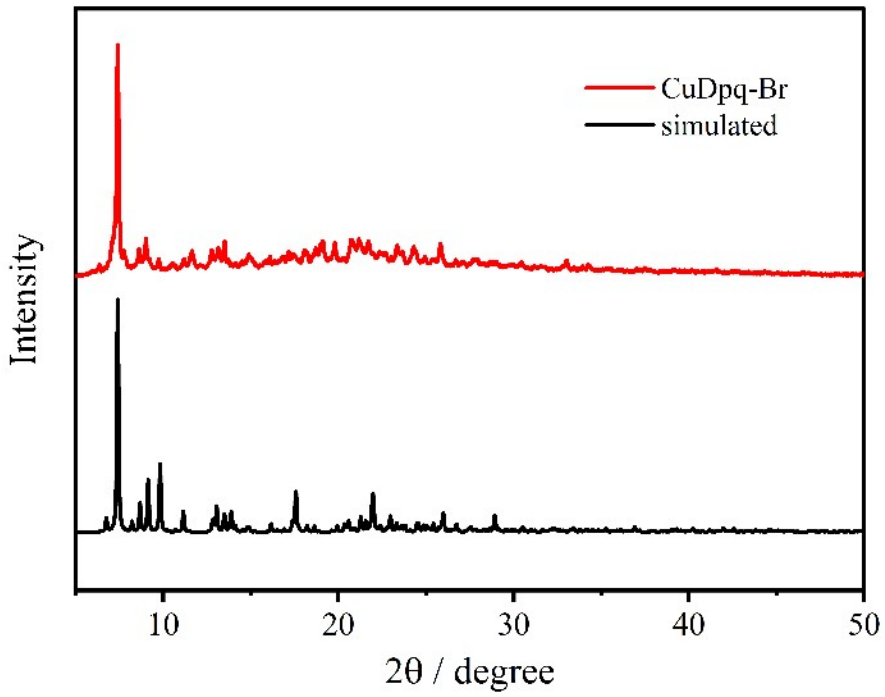

Fig. S30 The PXRD patterns for complex **2b**: simulated from single crystal data (Black) and single phase polycrystalline sample (Red).

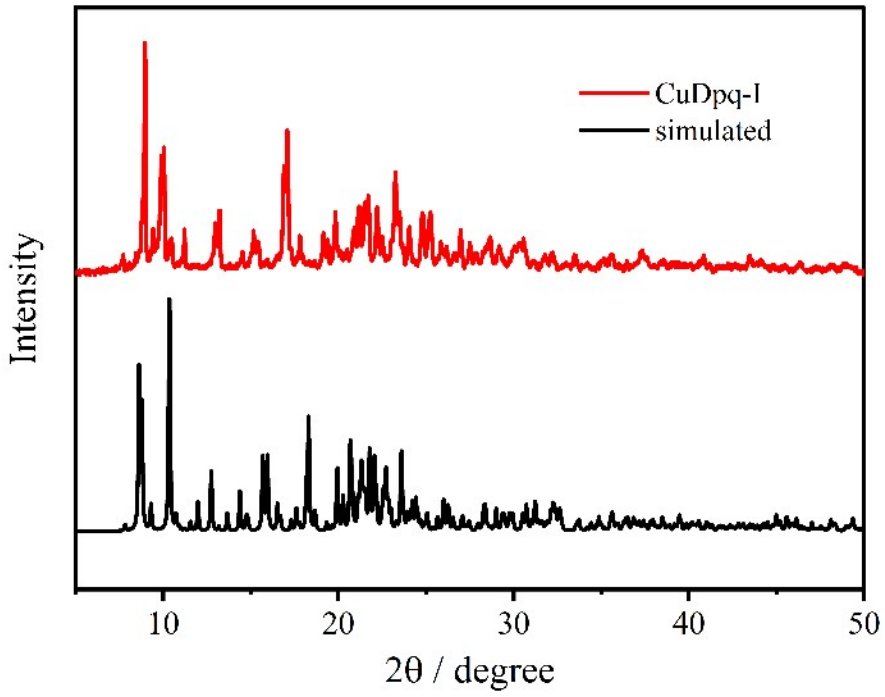

Fig. S31 The PXRD patterns for complex **3b**: simulated from single crystal data (Black) and single phase polycrystalline sample (Red).

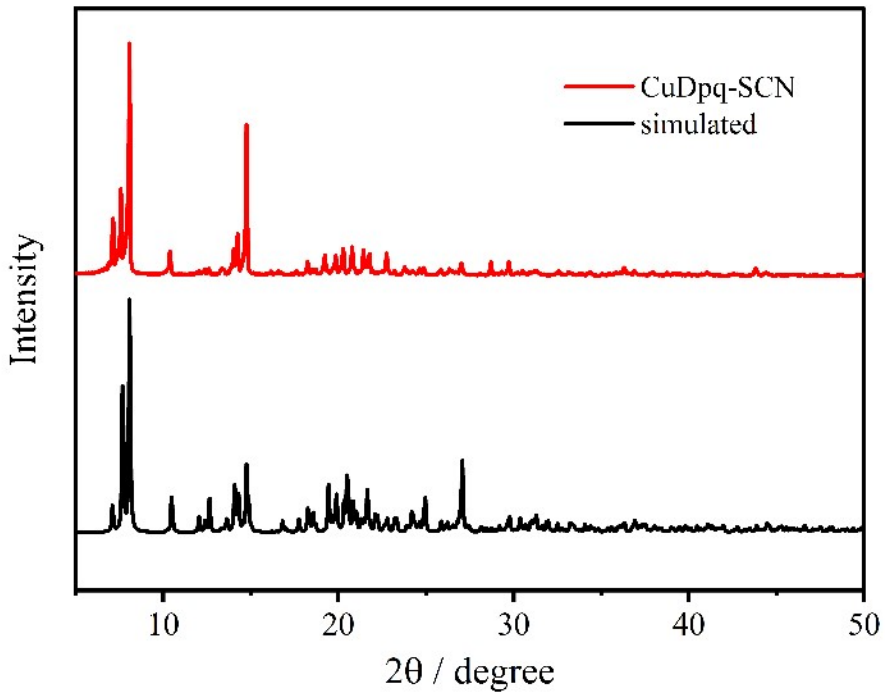

Fig. S32 The PXRD patterns for complex **4b**: simulated from single crystal data (Black) and single phase polycrystalline sample (Red).

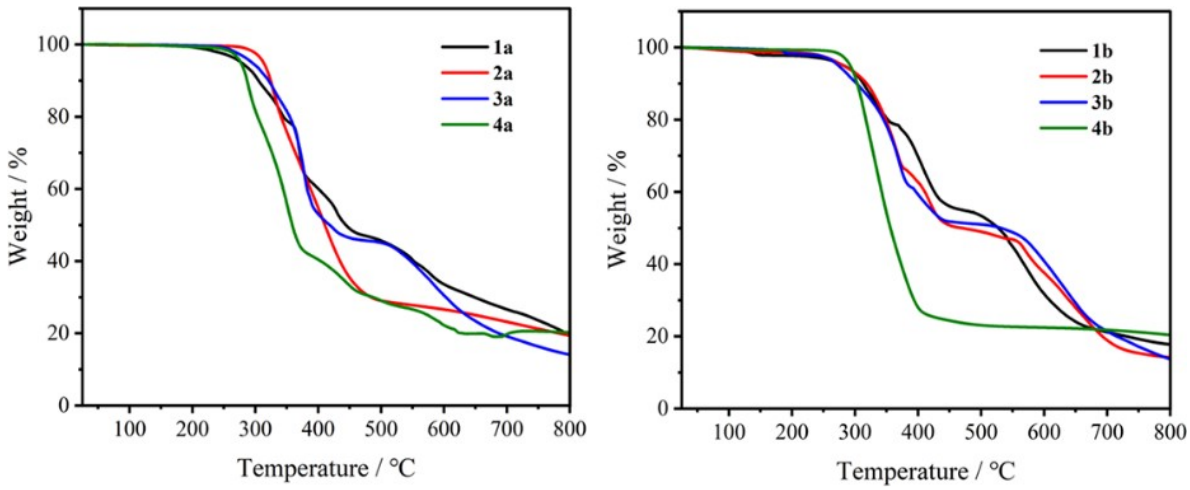

Fig. S33 The thermal stability curves for complexes **1a-4a** and **1b-4b**.

Table. S1 Selected bond lengths (Å) and angles (°) for complexes **1a-4a** and **1b-4b**.

1a			
Cu(1)-P(1)	2.2396(8)	P(2)-Cu(1)-P(1)	104.61(3)
Cu(1)-P(2)	2.2258(7)	N(4)-Cu(1)-P(1)	116.04(6)
Cu(1)-N(4)	2.044(2)	N(4)-Cu(1)-P(2)	110.13(6)
Cu(1)-N(3)	2.065(2)	N(4)-Cu(1)-N(3)	81.70(9)
		N(3)-Cu(1)-P(1)	124.31(6)
		N(3)-Cu(1)-P(2)	118.31(6)
2a			
Cu(1)-P(2)	2.2396(6)	P(1)-Cu(1)-P(2)	104.71(2)
Cu(1)-P(1)	2.2271(6)	N(2)-Cu(1)-P(2)	125.66(6)
Cu(1)-N(2)	2.0611(19)	N(2)-Cu(1)-P(1)	117.72(5)
Cu(1)-N(1)	2.062(2)	N(2)-Cu(1)-N(1)	81.46(8)
		N(1)-Cu(1)-P(2)	115.68(6)
		N(1)-Cu(1)-P(1)	109.44(6)
3a			
Cu(1)-P(1)	2.2354(7)	P(2)-Cu(1)-P(1)	105.02(3)
Cu(1)-P(2)	2.2269(8)	N(1)-Cu(1)-P(1)	127.53(7)
Cu(1)-N(1)	2.050(2)	N(1)-Cu(1)-P(2)	116.88(7)
Cu(1)-N(2)	2.070(2)	N(1)-Cu(1)-N(2)	81.39(9)
		N(2)-Cu(1)-P(1)	114.73(7)
		N(2)-Cu(1)-P(2)	108.34(7)
4a			
Cu(1)-P(1)	2.2306(5)	P(1)-Cu(1)-P(2)	105.026(18)
Cu(1)-P(2)	2.2350(5)	N(1)-Cu(1)-P(1)	118.66(4)

Cu(1)-N(1)	2.0462(14)	N(1)-Cu(1)-P(2)	126.66(4)
Cu(1)-N(2)	2.0685(14)	N(1)-Cu(1)-N(2)	81.61(6)
		N(2)-Cu(1)-P(1)	107.71(4)
		N(2)-Cu(1)-P(2)	113.81(4)
1b			
Cu(1)-P(1)	2.2522(10)	P(2)-Cu(1)-P(1)	105.31(4)
Cu(1)-P(2)	2.2347(9)	N(3)-Cu(1)-P(1)	119.12(7)
Cu(1)-N(3)	2.064(2)	N(3)-Cu(1)-P(2)	124.58(8)
Cu(1)-N(4)	2.079(3)	N(3)-Cu(1)-N(4)	80.28(10)
		N(4)-Cu(1)-P(1)	107.49(8)
		N(4)-Cu(1)-P(2)	117.36(8)
2b			
Cu(1)-P(2)	2.2525(7)	P(2)-Cu(1)-P(1)	105.30(3)
Cu(1)-P(1)	2.2414(7)	N(1)-Cu(1)-P(2)	119.72(6)
Cu(1)-N(1)	2.066(2)	N(1)-Cu(1)-P(1)	124.31(6)
Cu(1)-N(2)	2.086(2)	N(1)-Cu(1)-N(2)	80.09(8)
		N(2)-Cu(1)-P(2)	108.11(6)
		N(2)-Cu(1)-P(1)	116.55(6)
3b			
Cu(1)-P(1)	2.2229(7)	P(1)-Cu(1)-P(2)	102.67(3)
Cu(1)-P(2)	2.2515(7)	N(2)-Cu(1)-P(1)	127.83(6)
Cu(1)-N(2)	2.078(2)	N(2)-Cu(1)-P(2)	115.91(6)
Cu(1)-N(1)	2.056(2)	N(1)-Cu(1)-P(1)	123.32(7)
		N(1)-Cu(1)-P(2)	104.01(7)
		N(1)-Cu(1)-N(2)	80.89(9)
4b			
Cu(1)-P(1)	2.2335(6)	P(1)-Cu(1)-P(2)	102.97(2)
Cu(1)-P(2)	2.2494(6)	N(1)-Cu(1)-P(1)	116.58(5)
Cu(1)-N(1)	2.0472(17)	N(1)-Cu(1)-P(2)	123.12(5)
Cu(1)-N(2)	2.0971(17)	N(1)-Cu(1)-N(2)	80.22(7)
		N(2)-Cu(1)-P(1)	123.39(5)
		N(2)-Cu(1)-P(2)	110.92(5)

Table. S2 Intermolecular weak interactions for complexes **1a-4a** and **1b-4b**.

	Cg(i)/C-H→Cg(i)/(A)	Cg	Symmetry code	Cg(A)/H···Cg(B) / Å
1a	Cg(10)···Cg(10)	C35-C36-C39-C40-C38-C37	-x, -y, 1-z	3.9928
	C7-H7A→Cg(3)	N2-C1-C2-C3-C4-C5	1-x, 1-y, -z	2.95
	C24-H24→Cg(10)	C35-C36-C39-C40-C38-C37	-x, 1-y, 1-z	2.96

	C34-H34→Cg(7)	C14-C15-C16-C17-C18-C19	-x, -y ,1-z	2.89
	C15-H15···Cl1	/	/	2.77
	C29-H29···Cl1	/	1-x, 1-y, 1-z	2.77
	C43-H43···Cl1	/	/	2.68
2a	Cg(6)···Cg(6)	C4-C5-C6-C7-C12-C11	1-x, 1-y, 1-z	3.9368
	C8-H8→Cg(10) [i]	C38-C39-C40-C41-C42-C43	1-x, 1-y, 1-z	2.93
	C18-H18A→Cg(5) [ii]	N3-C13-C14-C15-C16-C17	-x, -y, 2-z.	2.99
	C1-H1···Br1 [i]	/	-x, 1-y, 1-z	2.84
	C28-H28A···Br1	/	x, -1+y, z	2.93
	C43--H43···Br1		-x, 1-y, 1-z	2.92
3a	Cg(6)···Cg(6)	C4-C5-C6-C7-C11-C12	1-x, 1-y, 1-z	3.8269
	C8-H8→Cg(10) [i]	C38-C39-C40-C41-C42-C43	1-x, 1-y, 1-z	2.92
	C14-H14→Cg(8)	C19-C20-C21-C22-C23-C24	1-x, -y, 1-z	2.97
	C1-H1···I1	/	/	3.01
4a	Cg(6)···Cg(6)	C4-C5-C6-C7-C12-C11	1-x, -y, -z	3.5830
	C12-H12→Cg(9) [i]	C32-C33-C34-C35-C36-C37	1-x, -y, -z	2.93
	C18-H18A→Cg(5) [ii]	N4-C13-C14-C15-C16-C17	-x, 1-y, 1-z	2.99
	C23-H23→Cg(8) [iii]	C25-C26-C27-C28-C29-C30	1-x, 1-y, -z	2.83
	C3-H3···N5	/	1-x, -y, -z	2.36
	C15-H15···S1	/	1-x, 1-y, 1-z	2.78
	C22-H22···S1	/	1-x, 1-y, -z	2.86
1b	O1-H1-Cl1	/	/	2.36
	O2-H2-Cl1	/	/	2.29
	O3-H3-Cl1	/	1-x, 1-y, 1-z	2.28
	C32-H32···O2	/	-1+x, y, z	2.33
	C33-H33···O1	/	-1+x, y, z	2.59
	C41-H41···O3	/	1/2+x, 1/2-y, 1/2+z	2.60
2b	C42-H42···O46	/	/	2.56
	C43-H43···O47	/	/	2.26
	O3-H3A···Br1	/	-1/2+x, 3/2-y, 1/2+z	2.68
	O46-H46A···Br1	/	/	2.55
	O47-H47···Br1	/	/	2.56
3b	C13-H13→Cg(10) [i]	C34-C35-C36-C37-C38-C39	1-x, 2-y, 1-z	2.86
	C17-H17→Cg(8) [ii]	C21-C22-C23-C24-C25-C26	1+x, y, z	2.79
	C24-H24→Cg(6)	N6-C15-C16-C17-C18-C19	1-x, 2-y, -z	2.90
	C1-H1···I1 [i]	/	/	3.00
4b	Cg(7)···Cg(7)	C4-C5-C6-C7-C12-C11	1-x, 1-y, 1-z	3.9801
	C14-H14→Cg(10) [i]	C34-C35-C36-C37-C38-C39	1-x, 1-y, 1-z	2.89

C33-H33A···S1 [i]	/	x, -1+y, z	2.78
C42-H42···N7 [ii]	/	1-x, 1-y, 1-z	2.60

Table. S3 Fluorescence data for ligands phen, Dpq and bdppmapy.

ligands	λ_{ex} / nm	λ_{em} / nm
phen	365	384
Dpq	382	419
bdppmapy	380	433

Table. S4 Energy, oscillator strength and major contribution of the calculated transitions for complexes **3a** and **3b**

Excited state	Energy	Oscillator strength	Contribution %	
$[Cu(bdppmapy)(phen)]^+$	5.1490 eV	0.1695	HOMO-17 -> LUMO	9.57
absorbtion	240.79 nm		HOMO-17 -> LUMO+2	3.48
			HOMO-9 -> LUMO+2	3.16
			HOMO-8 -> LUMO+2	**46.32**
			HOMO-5 -> LUMO+2	9.11
			HOMO-4 -> LUMO+2	3.96
$[Cu(bdppmapy)(phen)]^+$	2.7530 eV	0.0541	HOMO-5 -< LUMO	4.47
emission	450.36 nm		**HOMO-3 -< LUMO**	**59.03**
			HOMO-2 -< LUMO	23.19
			HOMO-1 -< LUMO+1	2.16
			HOMO -< LUMO+2	3.82
$[Cu(bdppmapy)(Dpq)]^+$	4.8957 eV	0.5546	HOMO-17 -> LUMO	9.29
absorbtion	253.25 nm		**HOMO-17 -> LUMO+2**	**39.42**
			HOMO-16 -> LUMO	12.81
			HOMO-16 -> LUMO+2	12.76
			HOMO-3 -> LUMO+4	2.88
$[Cu(bdppmapy)(Dpq)]^+$	2.6185 eV	0.0445	HOMO-3 -< LUMO	10.14
emission	473.49 nm		**HOMO-2 -< LUMO**	**70.56**
			HOMO-1 -< LUMO	12.08